ELSEVIER

Wear xxx (2004) xxx–xxx

WEAR

www.elsevier.com/locate/wear

Effect of crystallographic orientation on wear of diamond tools for nano-scale ductile cutting of silicon

M. Sharif Uddin, K.H.W. Seah*, X.P. Li, M. Rahman, K. Liu

Department of Mechanical Engineering, National University of Singapore, 9 Engineering Drive 1, Singapore 117576, Singapore

Received 26 November 2003; received in revised form 16 March 2004; accepted 16 March 2004

Abstract

Wear in diamond tools is a crucial factor in ultra-precision machining. However, as is well known, single crystal diamond possesses strong anisotropy. Its mechanical and physical properties vary with crystallographic orientation. In this study, tool wear investigation was carried out on nano-scale ductile cutting of silicon using an ultra-precision lathe with single crystal diamond tools. The wear characteristics of single point diamond tools and the effect of diamond crystallographic orientation were investigated. Experimental results indicate that gradual wear occurred mainly on the flank face of the tool. A very smooth wear mark on the rake face was also seen. The machining data show that wear resistance of the tool and tool life were greater when the crystallographic orientation of the rake face was {1 1 0} than when it was {1 0 0} or {1 1 1}. The thrust force on the diamond tool was lower when the rake face crystallographic orientation was {1 1 0} than when it was some other orientation. For all the crystallographic orientations studied in the diamond tools, gradual tool flank wear had no significant effect on the surface roughness of machined silicon work material.

Keywords: Single crystal diamond; Tool wear; Crystallographic orientation; Ductile cutting; Silicon

1. Introduction

With the recent advances in ultra-precision machining, single crystal diamond cutting is considered to be a sophisticated and pragmatic approach in industrial manufacturing applications. As single crystal diamond tools possess excellent mechanical properties such as extreme hardness, they can achieve very sharp cutting edges, crucial for machining precision components [1,2]. With the aid of this diamond turning technology, ductile mode cutting is a new approach to achieve superior surface finish along with minimum fractures of brittle workpiece materials such as silicon [3–6]. Through the ductile cutting, silicon can be deformed plastically with a machining scale of the order of a few tens of nanometers, resulting in sufficient hydrostatic pressure within the cutting region.

However, wear in single crystal diamond tools is an influential factor which not only raises the machining cost but also limits the cutting performance [7]. The tool wear problems become more severe particularly when the cutting edge radius is large. Additionally, it is well known that single crystal diamond is anisotropic; its mechanical and physical properties such as wear resistance, micro-strength, frictional coefficient, etc. vary not only with different crystallographic planes but also with different directions on the same crystallographic plane. A comprehensive study on the properties of diamonds done by Field [8] showed that the coefficient of friction of the {1 0 0} crystallographic plane is higher than that on the {1 1 0} plane and hence the {1 0 0} plane is softer than the {1 1 0} plane. However, the activation energy of the {1 0 0} plane is greater than that of the {1 1 0} plane, which indicates that at higher temperature, the {1 0 0} plane is more stable than the {1 1 0} plane.

In the discussion that ensues, we shall denote a crystallographic plane by { } and the direction of cutting/sliding as ⟨ ⟩. In terms of cleavage fracture along the {1 1 1} plane and tensile fracture, Wilks and Wilks [9] reported that the {1 0 0} crystallographic plane possesses higher strength compared to the {1 1 0} and {1 1 1} crystallographic planes. They also studied abrasion resistance of diamond surfaces with {1 0 0}, {1 1 0} and {1 1 1} crystallographic planes as a function of the azimuthal angle, and illustrated that the wear rates in the {1 0 0} ⟨1 0 0⟩, {1 1 0} ⟨1 0 0⟩ and {1 1 1} ⟨1 1 $\bar{2}$⟩ crystallographic directions are higher than those in the {1 0 0} ⟨1 1 0⟩, {1 1 0} ⟨1 1 0⟩ and {1 1 1} ⟨$\bar{1}$ $\bar{1}$ 2⟩ crystallographic directions. In addition, the cutting edge quality of a diamond

* Corresponding author. Tel.: +65-10-65-772-2212; fax: +65-10-65-772-1459.
E-mail address: mpeskh@nus.edu.sg (K.H.W. Seah).

0043-1648/$ – see front matter © 2004 Elsevier B.V. All rights reserved.
doi:10.1016/j.wear.2004.03.012

tool depends on the process of polishing, which in turn depends on the crystallographic orientation of the diamond surface. Due to this strong anisotropic nature in diamond, it can be expected that the rake face and flank face of a diamond tool having different crystallographic orientations can exhibit variations in wear progression and characteristics during actual machining operations.

Much research has previously been carried out to investigate diamond tool wear characteristics during machining with different workpiece materials, demonstrating that the severity and mechanism of wear in diamond tools vary with the type of workpiece material [10,11]. In observing diamond tool wear, Keen [12] proposed that fracture of the cutting edge and micro-grooving are the critical damage phenomena. He also observed the crystallographic orientation effects on wear resistance of diamond tools. Using 154 different diamond tools, Wong [13] characterized the major diamond failure modes as normal wear, chipping, chip dragging and fracture at the cutting edge by inclusions in work material, but found no significant effect of the crystallographic orientation on the tool performance during machining of aluminum. In another work done by Bex [14], it was found that besides gradual flank wear, tools with the flank oriented on the $\{1\,0\,0\}$ plane have a wear rate one-sixth that of tools with the flank oriented on the $\{1\,1\,0\}$ plane. Casey and Wilks [15] performed tool wear experiments on LM13 (an aluminum alloy with 12% silicon) using six single crystal diamond tools; three tools with $\{1\,0\,0\}$ as the rake plane and three tools with $\{1\,1\,0\}$ as the rake plane. They observed that tools with $\{1\,0\,0\}$ as the rake plane, show higher tool life by a factor of 7 compared to tools with other crystallographic orientations. However, to determine the cutting results in terms of cutting force and friction between tool and workpiece, Uegami et al. [16] held a different view for machining aluminum alloy, that is, diamond tools with $\{1\,1\,0\}$ as the rake face and cutting in the $\langle 1\,0\,0\rangle$ direction exhibit lower cutting forces and lower tool-chip friction compared to those with $\{1\,0\,0\}$ or $\{1\,1\,1\}$ as rake faces.

The research literature reviewed above, regarding tool failure modes as well as the effect of crystallographic orientation, involves the wear of diamond tools in the traditional machining of non-ferrous materials. Since diamond tool wear affects the surface quality in ductile cutting of silicon wafers, it is important to understand the quantitative wear progression as well as the wear mechanism with respect to cutting distance. Moreover, finding the relationship between wear characteristics and crystallographic orientations is a crucial factor in ductile cutting for minimizing tool wear and for selecting the optimum crystallographic plane of diamond tools. However, to date, there is little or no available literature documenting the effects of diamond crystallographic orientation on wear quantity and wear characteristics during nano-scale ductile cutting of brittle materials such as silicon.

This paper attempts to present and illustrate the wear progression characteristics and the wear mechanism of single crystal diamond tools during single point diamond turning of silicon in ductile mode. A relationship between wear resistance and crystallographic orientation of diamond tools has been proposed and discussed.

2. Experimental set-up

2.1. Equipment used

In this study, a TOSHIBA ultra-precision lathe (ULG-100) comprising an air-bearing spindle and an air slide with a capacity of 1 nm positioning accuracy was used. A Scanning electron microscope (SEM) (JEOL Ltd., JSM-5500) was used to examine the tool cutting edge, machined surface and chips produced. A Nomarski optical microscope (OLYMPUS STM-6) was used to measure the flank wear of cutting tools. The micro-cutting forces during tool wear experiments were measured using a KISTLER Mini-3-D Dynamometer (Type-9256A) in conjunction with a KISTLER 3-Channel charge amplifier and a SONY digital recorder. Fig. 1 shows a schematic diagram of two major cutting force components such as cutting force F_c and thrust force F_t acting at the tool tip during machining. The surface roughness of the machined silicon workpiece was measured using a Mitutoyo FORMTRACER (CS-5000). Five points were selected for surface roughness measurement and the average value was calculated and recorded. Before machining, indentation tests (IT) [17] of the cutting tools were done, and the cutting edge radius was estimated using an Atomic force microscope (AFM) (S.I.I., SPA-500).

2.2. Cutting tools and work materials

Three round-nosed single crystal synthetic diamond tools, which have different crystallographic orientations, were used for tool wear experiments in this study. All the diamond tools used in the tests were commercially available from Tokyo Diamond Industries (TDI) Ltd., Japan. The crystallographic orientations and basic geometrical parameters of diamond tools used are summarized in Table 1. Fig. 2 shows

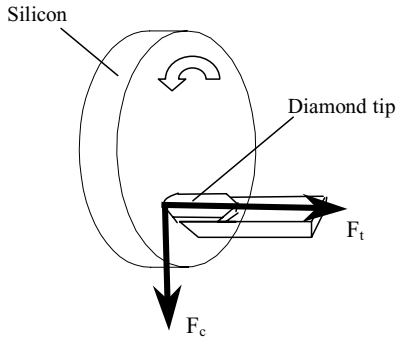

Fig. 1. Micro-cutting forces acting at the cutting tool point.

Table 1
Crystallographic orientations and geometry of the tested diamond tools

Tool's material	Single crystal synthetic diamond
No. of tools	Crystallographic orientations
Tool-1	{1 1 0} as rake and {1 0 0} as flank
Tool-2	{1 0 0} as rake and {1 0 0} as flank
Tool-3	{1 1 1} as rake and {1 1 2} as flank
Tool's geometry	
Nose radius (mm)	2
Rake angle (°)	0
Clearance angle (°)	7
Cutting edge radius (nm)	~30–60
Inclination of crystal orientation (°)	~5–6

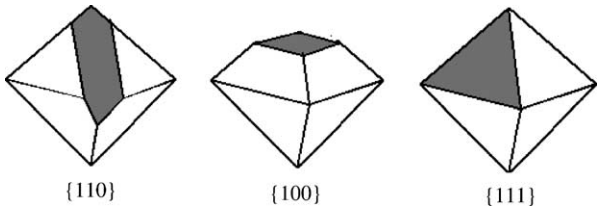

Fig. 2. Schematic representation of different diamond crystallographic orientations.

the schematic representation of typical diamond crystallographic orientations for different diamond shapes. Before the tool wear experiments, the main cutting edge of a diamond tool appears to be smooth and sharp revealing no visible defects under higher magnification, as can be seen in Fig. 3.

Commercial single crystal silicon wafer having {1 1 1} crystallographic orientation was used as the work material. The reason for choosing the {1 1 1} crystallographic plane is that this plane possesses the lowest cleavage energy at the shear zone. The silicon workpiece is 100 mm in diameter and 0.65 mm thick. Table 2 lists the physical and mechanical properties of single crystal silicon at room temperature [18,19]. The silicon wafers were bonded onto diamond turned aluminum blanks using heat-softened glue and then vacuum chucked on the machine spindle. Before performing the cutting test, the silicon surfaces were machined using other diamond tools to get a mirror-like surface, the roughness value (R_a) of which ranges from several microns to the order of nanometers.

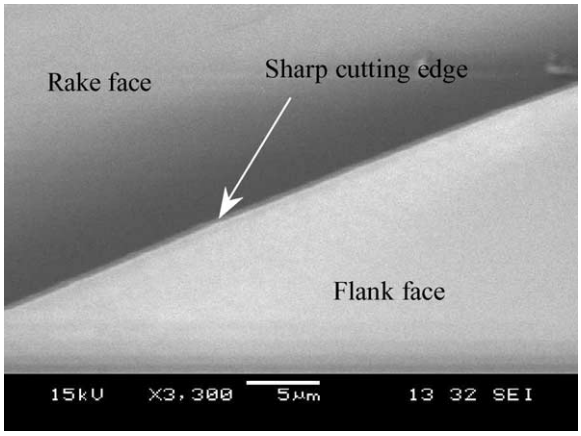

Fig. 3. SEM photograph of the main cutting edge of a diamond tool.

Table 2
Properties of single crystal silicon

Material property	Value[a]	Value[b]	Average
Density, ρ (g/cm^3)	2.328	2.33	2.329
Melting point, T_m (°C)	1420	1410	1415
Young's modulus, E (GPa)	131	155.8	143.4
Fracture toughness, K_c (MPa m$^{1/2}$)	0.9	0.6	0.75
Shear modulus, G (GPa)	79.9	64.10	72
Poisson's ratio, ν	0.266	0.2152	0.2406
Vicker's hardness, H_v (kg/mm^2)	1000	1000	1000

[a] Ref. [18].
[b] Ref. [19].

2.3. Cutting conditions

Face-turning operations were carried out and the cutting parameters shown in Table 3 were used for three diamond tools of different crystallographic orientations throughout the cutting experiments. The surface cutting speed was kept constant by adjusting the rotational speed. The other cutting parameters such as feed rate and depth of cut were selected based on parametric studies of ductile mode cutting of brittle materials. All the cutting experiments were conducted in a dry environment to ensure proper chip collection.

2.4. Ductile cutting and maximum undeformed chip thickness

For nano-scale ductile cutting of brittle materials, as undeformed chip thickness varies from zero at the tool tip center to a maximum value at the top of uncut shoulder, it is very important to determine quantitatively the maximum undeformed chip thickness which must be smaller than the cutting edge radius of the tools [3]. Fig. 4 represents a schematic diagram of maximum undeformed chip thickness in the ductile cutting of silicon work materials. From the figure, it is seen that O_1 and O_2 are the centers of two adjacent arc cutting edges, and the distance between O_1 and O_2 is the feed rate used in the cutting experiments. Using geometrical analysis of Fig. 4, the maximum undeformed chip thickness in a

Table 3
Experimental cutting parameters (errors within ±0.1%)

Parameters	Value
Cutting speed (m/min)	185.35
Feed rate (nm/rev)	100
Depth of cut (μm)	1
Undeformed chip thickness (nm)	3.159
Cutting environment	Dry

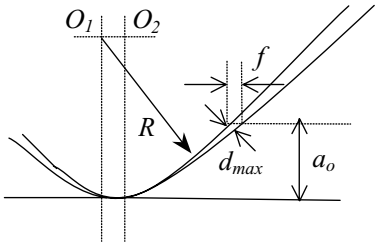

Fig. 4. Schematic diagram of maximum undeformed chip thickness for small feed rate ($\sqrt{2Ra - a^2} > f$).

nanometer level can be obtained by arranging combinations of the tool nose radius R, the depth of cut a_0 and the feed rate f. Hence, based on our cutting parameters and satisfying the condition $\sqrt{2Ra_0 - a_0^2} > f$ for small feed rate, the maximum undeformed chip thickness $d_{\max}$ was calculated to be 3.195 nm using the following equation:

$$d_{\max} = R - (R^2 + f^2 - 2f(2a_0R - a_0^2)^{1/2})^{1/2} \quad (1)$$

3. Results and discussion

3.1. Wear patterns and mechanisms

Ductile cutting tool wear tests were performed using a diamond tool having the crystallographic plane {1 1 0} as rake face. The wear region of the diamond tool was monitored at certain cutting distances. Fig. 5 is an SEM (scanning electron microscopy) photograph of the cutting edge of the diamond tool after cutting for 2.15 km. A very small-scale wear on the flank region was observed and nearly the whole mid-zone of the cutting edge showed greater wear. A microscopic ruggedness on the cutting edge was also seen. After cutting for 3.36 km, as shown in Fig. 6, the wear region exhibits gradual flank wear as well as some micro-grooves on the flank, which are on the average 5 mm in length. It was also seen that micro-grooves larger in height lie approximately at the mid-point of the cutting edge length.

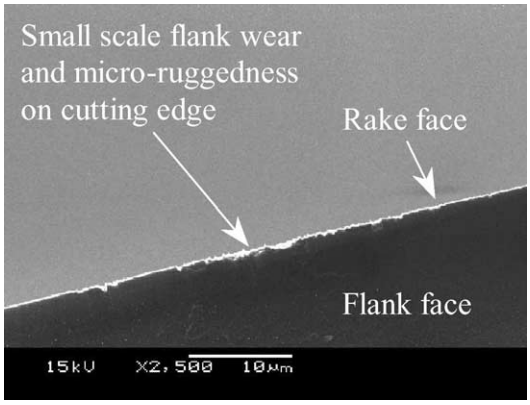

Fig. 5. SEM photograph of flank wear region after cutting for 2.15 km.

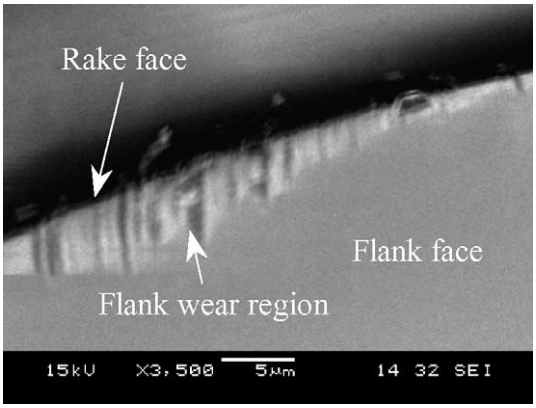

Fig. 6. SEM photograph of flank wear region after cutting for 3.36 km.

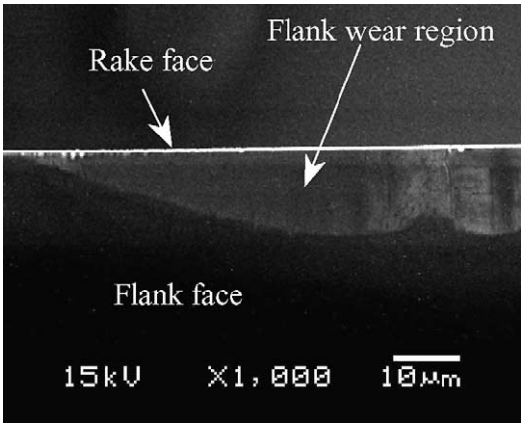

Fig. 7. SEM photograph of flank wear region after cutting for 10 km.

Fig. 7 shows the diamond tool wear region after cutting for 10 km. Gradual flank wear was seen to dominate. Additionally, the wear zone increased in height and width without further formation of micro-grooves in the flank wear region. However, a very smooth wear mark on the rake surface of the tool was observed after cutting for 10 km, as shown in Fig. 8. The width (KB) of the wear mark was found

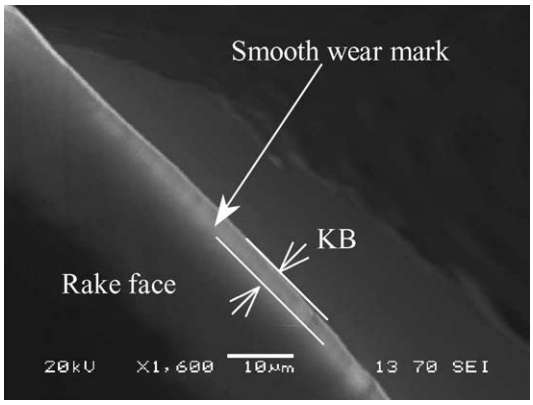

Fig. 8. SEM photograph of rake face of diamond tool after cutting for 10 km.

to be 3.35 mm along the effective cutting edge length of the tool.

In ultra-precision machining, diamond tool wear was a subject of controversy [9–12]. Its mechanism is not understood clearly even till today. Although several different mechanisms are involved in diamond tool wear, some of which may be involved only under certain circumstances, the predominant wear will depend on the cutting conditions used in the tests.

During ductile cutting or cutting at an undeformed chip thickness of a nano-level, the basic tool wear occurrence is likely to be a gradual process. This can be due to the combined actions of mechanical abrasion wear and adhesion wear. At the start of a cutting test, since the tool is very sharp, the stresses on the tool cutting edge are very severe, resulting in a micro-ruggedness on the cutting edge. Besides, the silicon surface may not be perfectly flat, the shear deformation occurring at varying depths of cut on the silicon surface during machining even if a constant depth of cut was planned. This can lead to some micro-grooves on the flank region along with increasing gradual flank wear. As the cutting distance increases, the cutting edge undergoes recession and the flank wear region becomes predominant. The flank wear region then causes a reduction in clearance angle, which gives rise to increased frictional resistance and cutting forces.

However, during nano-scale ductile cutting of brittle materials, the undeformed chip thickness varies from zero at the tool center tip to a maximum value at the top of the uncut shoulder; a 'zero-cutting zone' exists within which no chips are produced. In this special zone, the tool acts more like a roller than a cutter and continuously slides on and burnishes the machined surface. This could be another reason for a relatively higher flank wear progression of the tool near the center of the tool. This wear rate increases drastically as the temperature of this zone reaches the thermo-chemical deterioration point of diamond [20]. This kind of wear may involve graphitization of the diamond tool, aggravated by the chemical affinity between carbon, silicon and the oxygen in the ambient air [21].

In traditional cutting, it has been found that wear on the rake face results from the severe effect of chip flow characteristics. However, when cutting at a nano-level of undeformed chip thickness, i.e. with very low material removal rate, the effect of chip flow on the rake face is considerably less. This could be a possible reason for the very smooth wear mark on the rake face during ductile cutting of silicon.

3.2. Quantitative tool wear and cutting distance

With the growing concern in the tool wear effect on machined surface roughness in ductile cutting, it is necessary to predict the trend of tool wear progression with respect to cutting distance. Since the dominant wear was tool flank wear, which increases in both height and width, the maximum dimension of wear height, VB_{max} and width were measured at various cutting distances. Fig. 9 shows a schematic diagram of typical flank wear and its measurement.

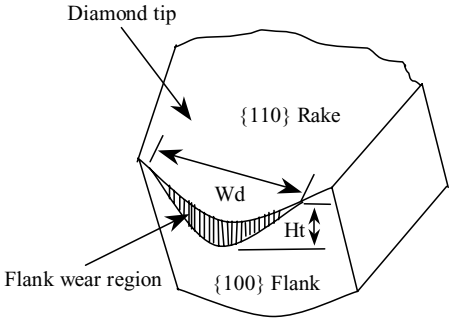

Fig. 9. Typical flank wear and it measurement for a diamond tool.

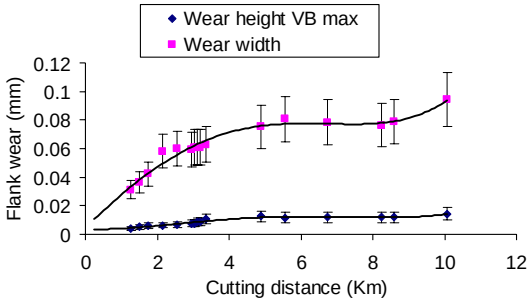

Fig. 10. Flank wear progression of diamond tool with {1 1 0} orientation as the rake face as a function of cutting distance.

Fig. 10 illustrates the behavior of tool flank wear with respect to cutting distance for diamond tool having {1 1 0} crystallographic orientation as the rake face. It is seen here that it is only after cutting for around 1.0 km that the diamond tool shows observable wear on its flank. Tool wear progression tends to be slow initially, but increases significantly after cutting for around 3.0 km. Flank wear width gets significantly more dominant with cutting distance, as compared with flank wear height VB_{max} (Fig. 10). After 10 km of cutting, the maximum flank wear height VB_{max} can be estimated to be 14 μm, which is not expected to severely affect the cutting performance. Here occurrence of progressive flank wear is basically caused by mechanical abrasion and adhesion between the cutting tool and the machined surface, and possible thermo-chemical effect as described in Section 3.1. Furthermore, with the increase in cutting distance, the wear, which begins at the tool tip, increases in height and width because the contact area between the cutting tool and work material increases, thus forming a greater wear region on the flank face.

3.3. Crystalline orientation and tool wear behavior

Given the highly anisotropic nature of single crystal diamond, its mechanical and physical properties vary with crystallographic orientation. Hence, it would seem desirable to specify certain crystallographic orientations which give

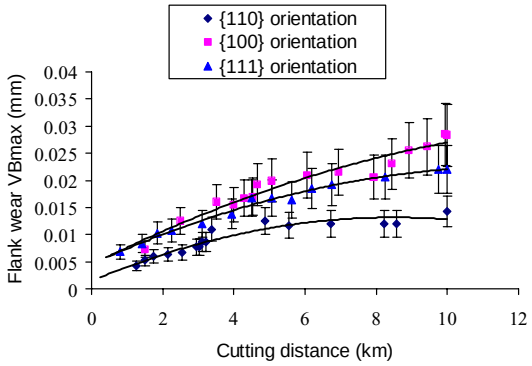

Fig. 11. Behavior of flank wear VB_{max} for three different crystallographic orientations.

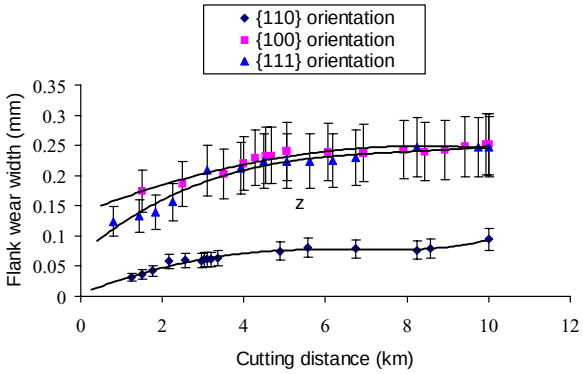

Fig. 12. Behavior of flank wear width for three different crystallographic orientations.

higher tool wear resistance. In view of this, under the same experimental cutting conditions (Table 3), nano-scale ductile cutting experiments using diamond tools of three different crystallographic orientations as the rake faces (Table 1) were performed, and flank wear with respect to cutting distance was measured, as plotted in Figs. 11 and 12. From these figures, it can be seen that although the wear patterns and mechanisms for all three crystallographic orientations are the same (Fig. 13(a)–(c)), the diamond tool with {1 1 0} crystallographic orientation as the rake face shows greater wear resistance than those with {1 0 0} and {1 1 1} crystallographic orientations as the rake faces. It is also seen that diamond tools with {1 0 0} and {1 1 1} crystallographic orientations as the rake faces exhibit very similar wear characteristics to one another with respect to cutting distance. Wear data presented in the above graphs reflect some fluctuations with the cutting distance. This could be due to the fact that as cutting distance increases, the reference cutting edge due to tool flank wear changes, thus leading to a lower wear value measured by a Nomarski optical microscope.

Experimental results indicate that in nano-scale machining of brittle materials, cutting edge recession and gradual flank wear are predominant. These are mainly due to the mechanical abrasion between the diamond tool and the silicon. Hence, analysis of tool wear considering the crystallographic orientation of flank is of greater concern in this section. The diamond tools with {1 1 0} and {1 0 0} as the rake faces both have {1 0 0} as the flank face (Table 1) but show different flank wear characteristics.

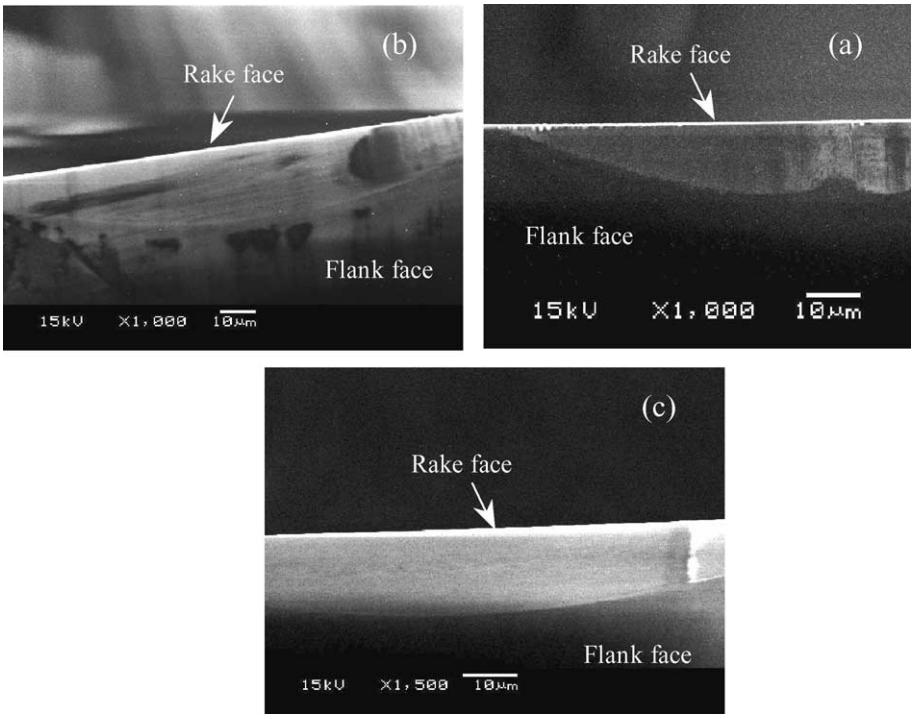

Fig. 13. SEM photographs of wear patterns of diamond tools with (a) {1 1 0}; (b) {1 0 0} and (c) {1 1 1} crystallographic orientations as the rake faces after cutting for 10 km.

Usually the relationship between wear rate and crystallographic orientation of diamonds depends on its background of polishing mechanisms and crystallographic orientations [22]. There could be an unavoidable difference between cutting wear rate and polishing rate because during actual machining, the cutting stress distribution is somewhat different from the stress distribution when a diamond surface is polished by a scaife. Furthermore, the cutting directions, namely harder and softer directions on a crystal plane, affect the tool wear rate [8]. Thus the harder direction ⟨1 1 0⟩ on the flank with {1 0 0} crystallographic orientation may possibly be responsible for less wear and longer tool life for diamond tools with {1 1 0} crystallographic orientation as the rake face. Also the higher wear rate and lower tool life for diamond tools with {1 0 0} and {1 1 1} crystallographic orientations as the rake faces may correspond to the softer directions ⟨1 0 0⟩ and $\langle 1\,1\,\bar{2}\rangle$ on the flanks with {1 0 0} and {1 1 2} crystallographic orientations.

Additionally, recent research work done on diamond polishing by van Bouwelen et al. [23], Grillo et al. [24], and Grillo and Field [25], suggest that wear debris produced when polishing diamond in the ⟨1 0 0⟩ direction on the {1 0 0} crystallographic plane (the soft direction or direction of higher wear rate) consists of carbon particles of lower density, indicating wear by a stress-induced phase change from diamond (sp^3) to graphite (sp^2), the latter being a form of carbon having a lower density. However, wear particles obtained after polishing in the ⟨1 1 0⟩ direction (hard direction or direction of low wear rate) on the same plane consist of fragments of diamond (sp^3), indicating material removal by a mechanical process of chipping on a microscopic scale. In actual machining, as the temperature at the tool–work interface increases with cutting time, wear due to a phase change from diamond (sp^3) to graphite (sp^2), is more severe in the soft direction ⟨1 0 0⟩ compared to in the hard direction ⟨1 1 0⟩. Hence, this difference in wear rate and mechanism with respect to crystallographic direction on the same plane may lead to greater wear resistance and tool life for diamond tools with {1 1 0} as the rake face compared to diamond tools with other rake face orientations.

The micro-strength and wear resistance of the cutting edge of a diamond tool, however, depend also on the combined effects of crystallographic orientations of both rake and flank faces. Hence, experimental results on tool wear obtained in this study are somewhat different from those obtained by Yuan et al. [26], Hurt and Decker [27], and the theoretical prediction made by Ikawa and Shimada [28]. However, our observations confirm experimental findings described by Oomen et al. [10]. It can thus be said that under some conditions, a diamond tool with {1 1 0} orientation as the rake face and {1 0 0} orientation as the flank face could show higher wear resistance during actual machining and hence this set of orientations can be a good choice of crystallographic plane selections for diamond tools.

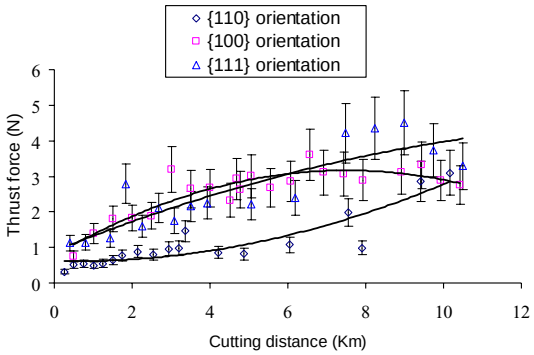

Fig. 14. Thrust force characteristics for three crystallographic orientations.

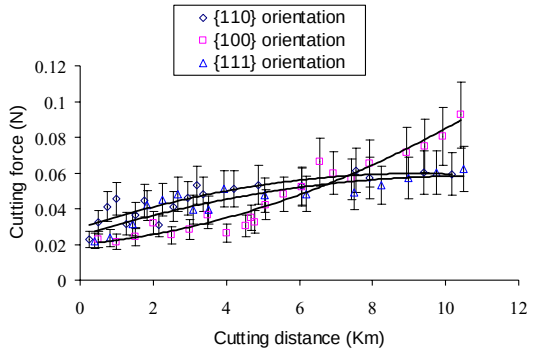

Fig. 15. Cutting force characteristics for three crystallographic orientations.

3.4. Crystalline orientations and micro-cutting forces

In this study, two major micro-cutting force components were observed, along with tool wear characteristics. Figs. 14–16, respectively, show the relationships between the thrust force F_t, the cutting force F_c, and the force ratio r (F_c/F_t) with respect to cutting distance for three different crystallographic orientations in diamond tools. It was found that in nano-scale ductile cutting of brittle materials with a diamond tool having a certain cutting edge radius, the effective rake angle causes the thrust force to be higher than the cutting force. Fig. 14 shows that the thrust force for a diamond tool with {1 1 0} crystallographic orientation as the rake face is much lower than those with the other two

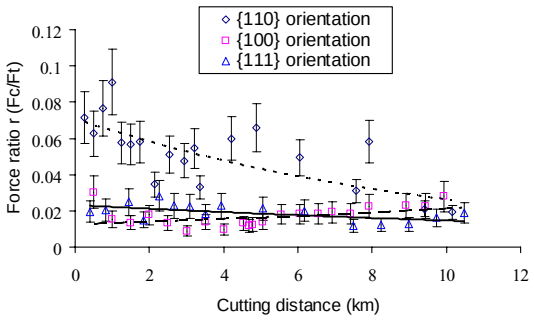

Fig. 16. Variation in force ratio r (F_c/F_t) for three crystallographic orientations.

crystallographic orientations as rake faces. The thrust force characteristics for diamond tools with {1 0 0} and {1 1 1} crystallographic orientations as the rake faces (Fig. 14) exhibit almost the same trend with respect to cutting distance. It can also be seen that after cutting for 10 km, the thrust force data for diamond tools with three crystallographic orientations lie within a narrow range. It can also be seen from Fig. 15 that the cutting force characteristics for diamond tools with {1 1 0} and {1 1 1} crystallographic orientations as the rake faces show a similar trend with respect to cutting distance. Moreover, the variation in cutting force data for diamond tools with all three crystallographic orientations is comparatively lower. Fig. 16 shows that although the force ratio (F_c/F_t) for the diamond tool with {1 1 0} as the rake face decreases monotonically with cutting distance, it is invariably higher than those for tools with {1 0 0} and {1 1 1} as the rake faces.

Traditionally, with increase in cutting distance, which is proportional to machining time, the tool flank wear height VB_{max} and width increase and hence, there is a natural and gradual increase in cutting forces. From our experimental results regarding micro-cutting forces (Figs. 14 and 15), it can be said that the predominantly lower tool wear characteristics for the diamond tool with {1 1 0} crystallographic orientation as the rake face may be the reason for significantly lower thrust force. Also, the similar thrust characteristics for diamond tools with {1 0 0} and {1 1 1} crystallographic orientations as the rake faces can be a result of the same tool wear progression of both these diamond tools (Figs. 11 and 12). For all three crystallographic orientations, the increase in cutting distance and tool wear does not have much effect on the cutting force except for a slight variation in cutting force in the case of the tool with {1 0 0} as the rake face. Moreover, our micro-cutting force observations in relation to crystallographic orientations agree with the experimental results obtained by Uegami et al. [16].

3.5. Crystalline orientations and surface roughness

Generally the surface roughness of machined work material depends on many factors such as tool wear, properties of the work material, and machining conditions. For instance, the tool wear, which was the output parameter studied primarily, is very much dependent on cutting distance assuming other factors are held constant. The influence of the cutting distance on the surface roughness of silicon machined using diamond tools with three crystallographic orientations is shown in the graphs in Figs. 17 and 18. From these graphs, it can be seen that for the three crystallographic orientations, the surface roughness parameters R_a (average) and R_y (peak-valley) of machined silicon are distributed randomly within a very short range and their variation lies between 2 and 4 nm, and between 9 and 22 nm, respectively.

It is likely that with increase in cutting distance and hence, in tool wear for the three crystallographic orientations, there

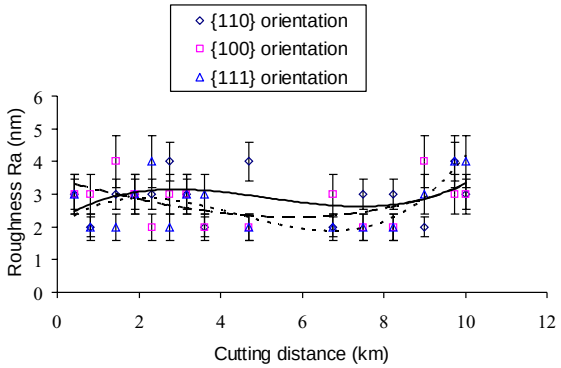

Fig. 17. Effect of cutting distance on average surface roughness R_a for three crystallographic orientations.

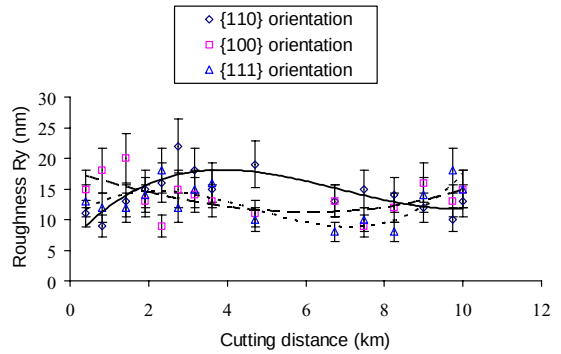

Fig. 18. Effect of cutting distance on surface roughness R_y (peak-valley) for three crystallographic orientations.

is no significant variation in surface roughness (R_a and R_y) of the machined workpiece in nano-scale ductile cutting of silicon. Such surface roughness characteristics could be due to the smooth surface structure of the gradual tool flank wear region (Fig. 13) and the experimental cutting conditions rather than the increased cutting distance.

4. Conclusions

The following conclusions can be drawn from our experimental results:

- Nano-scale ductile cutting of silicon using a single crystal diamond tool gives a very smooth wear mark on the tool rake face, and a much more severe wear at the flank.
- Regarding the effects of crystallographic orientation on diamond tool wear, it was found that a diamond tool with {1 1 0} crystallographic orientation as the rake face yields longer tool life and greater wear resistance compared to those with {1 0 0} and {1 1 1} crystallographic orientations as the rake faces.
- The thrust force for a diamond tool with {1 1 0} crystallographic orientation as the rake face is comparatively lower than those for diamond tools with {1 0 0} and {1 1 1} crystallographic orientations as the rake faces. However, the cutting force characteristics for all three rake face

crystallographic orientations have increasing trends with respect to cutting distance.

- For all three crystallographic orientations, the machined surface roughness values (R_a and R_y) do not vary significantly with the progress of tool flank wear.

Acknowledgements

The authors would like to thank Mr. See Cheng Wai, a final year undergraduate student, for his cooperation in performing the experiments.

References

[1] N. Iwaka, R.R. Donaldson, R. Kumanduri, W. Konig, P.A. Mckeown, T. Moriwaki, I.F. Stowers, Ultra-precision metal cutting—the past, the present and the future, Ann. CIRP 40 (2) (1991) 587–593.
[2] N. Ikawa, S. Shimada, H. Morooka, Technology of diamond tool for ultra-precision metal cutting, Bull. Jpn. Soc. Precis. Eng. 21 (4) (1987) 233–238.
[3] W.S. Blackley, R.O. Scattergood, Ductile regime model for diamond turning of brittle materials, J. Precis. Eng. 13 (2) (1991) 95–102.
[4] T. Shibata, S. Fujii, E. Makino, M. Ikeda, Ductile-regime turning mechanism of single-crystal silicon, J. Precis. Eng. 18 (1996) 129–137.
[5] T.P. Leung, W.B. Lee, X.M. Lu, Diamond turning of silicon substrates in ductile regime, J. Mater. Process. Technol. 73 (1998) 42–48.
[6] C.L. Chao, K.J. Ma, D.S. Liu, C.Y. Bai, T.L. Shy, Ductile behavior in single-point diamond-turning of single-crystal silicon, J. Mater. Process. Technol. 127 (2002) 187–190.
[7] J. Yan, K. Syoji, J. Tamaki, Some observations on the wear of diamond tools in ultra-precision cutting of single-crystal silicon, Wear 255 (2003) 1380–1387.
[8] J.E. Field (Ed.), The Properties of Diamond, Academic Press, London, 1979, pp. 281–324.
[9] J. Wilks, E. Wilks, Properties and Applications of Diamond, Butterworths, 1991.
[10] J.M. Oomen, J. Eisses, Wear of mono-crystalline diamond tools during ultra-precision machining of nonferrous metals, Precis. Eng. 14 (4) (1992) 206–218.
[11] R. Wada, H. Kodama, K. Nakamura, Wear characteristics of single crystal diamond tool, Ann. CIRP 29 (1) (1980) 47–52.
[12] D. Keen, Some observations of the wear of diamond tools used in piston machining, Wear 17 (1971) 195–208.
[13] C.J. Wong, Fracture and wear of diamond cutting tools, Trans. ASME J. Eng. Mater. Technol. 103 (1981) 341–345.
[14] P.A. Bex, Diamond turning tools, Ind. Diam. Rev. 1 (1975) 11–18.
[15] M. Casey, J. Wilks, Some experiments to study turning tools using the scanning microscope, Int. J. Mach. Tool Des. Res. 16 (1976) 13–22.
[16] K. Uegami, K. Tamamura, K.K. Jang, Lapping and frictional properties of diamond, and characteristics of diamond cutting tool, J. Mech. Work. Technol. 17 (1988) 147–155.
[17] X.P. Li, M. Rahman, K. Liu, K.S. Neo, C.C. Chan, Nano-precision measurement of diamond tool edge radius for wafer fabrication, J. Mater. Process. Technol. 140 (2003) 358–362.
[18] J.J. Wortman, R.A. Evans, Young's modulus, shear modulus, and Poisson's ratio in silicon and germanium, J. Appl. Phys. 36 (1) (1965) 153–156.
[19] W.A. Brantly, J. Appl. Phys. 44 (1) (1973) 534.
[20] K. Cheng, X. Luo, R. Ward, R. Holt, Modeling and simulation of the tool wear in nanometric cutting, Wear 255 (2003) 1427–1432.
[21] K.E. Puttick, L.C. Whitemore, P. Zhdan, A.E. Gee, C.L. Chao, Energy scaling transitions in machining by diamond, Tribol. Int. 28 (6) (1995) 349–355.
[22] E.M. Wilks, J. Wilks, The abrasion resistance of natural and synthetic diamond, Wear 81 (1982) 329–346.
[23] F.M. van Bouwelen, J.E. Field, L.M. Brown, Electron microscopy analysis of debris produced during diamond polishing, Phil. Mag. 83 (2003) 839–855.
[24] S.E. Grillo, J.E. Field, F.M. van Bouwelen, Diamond polishing: the dependency of friction and wear on load and crystal orientation, J. Phys. D: Appl. Phys. 33 (2000) 985–990.
[25] S.E. Grillo, J.E. Field, The polishing of diamond, J. Phys. D: Appl. Phys. 30 (1997) 202–229.
[26] Z.J. Yuan, J.C. He, Y.X. Yao, The optimum crystal plane of natural diamond tool for precision machining, Ann. CIRP 41 (1) (1992) 605–608.
[27] H.H. Hurt, D.L. Decker, Tribological considerations of the diamond single-point tool, in: Proceedings of SPIE, Production Aspects of Single-point Machine Optics, vol. 508, 1986, pp. 126–131.
[28] N. Ikawa, S. Shimada, Microfracture of diamond as fine tool material, Ann. CIRP 31 (1982) 71–74.